

R. E. Cohen and J. S. Weitz

Geophysical Laboratory and Center for High Pressure Research, Carnegie Institution of Washington,
Washington D.C. 20015

The Melting Curve and Premelting of MgO

Short title:

Abstract. The melting curve for MgO was obtained using molecular dynamics and a non-empirical, many-body potential. We also studied premelting effects by computing the dynamical structure factor in the crystal on approach to melting. The melting curve simulations were performed with periodic boundary conditions with cells up to 512 atoms using the ab-initio Variational Induced Breathing (VIB) model. The melting curve was obtained by computing ΔH_m and ΔV_m and integrating the Clapeyron equation. Our ΔH_m is in agreement with previous estimates and we obtain a reasonable ΔV_m , but our melting slope dT/dP (114 K/GPa) is three times greater than that of Zerr and Boehler [1994] (35 K/GPa), suggesting a problem with the experimental melting curve, or an indication of exotic, non-ionic behavior of MgO liquid. We computed $S(q, \omega)$ from simulations of 1000 atom clusters using the Potential Induced Breathing (PIB) model. A low frequency peak in the dynamical structure factor $S(q, \omega)$ arises below the melting point which appears to be related to the onset of bulk many-atom diffusive exchanges. These exchanges may help destabilize the crystalline state and be related to intrinsic crystalline instability suggested in earlier simulations.

Introduction

Understanding melting is crucial for understanding the evolution and dynamics of the Earth. In order to trace the development of the Earth from its origin until now, it is important to know the melting temperatures, enthalpy of melting, and density of melts and solids as functions of composition. There is also fundamental interest in understanding the melting process. Why and how do crystals melt, and are there any precursors to the melting transition evident in the crystalline phase? Here we are particularly interested in how pressure might effect melting and premelting behavior. Since we are interested in eventually understanding melting in the Earth, we start with the simplest oxide, MgO, and study its melting and premelting in the crystalline phase as a function of compression.

Measuring melting curves to extreme pressures is very difficult, and there have been significant discrepancies among laboratories on melting curves of the important geophysical materials Fe [*Anderson and Ahrens, 1996; Boehler, 1996*] and MgSiO₃ perovskite [*Heinz et al., 1994; 27; Sweeney and Heinz, 1993; Zerr and Boehler, 1993*]. It is also very difficult to calculate melting curves theoretically in spite of many attempts to develop predictive models for melting. Calculation of melting curves from fundamental physics is a difficult undertaking as well; difficult because accurate potentials or electronic structure methods are needed to obtain the forces among atoms, long simulations are needed to equilibrate and obtain thermodynamic properties of the liquid, and since free-energies cannot be directly calculated, one must perform thermodynamic integrations or reversals [*Cohen and Gong, 1994*] in order to obtain the melting point. The most widely applied method to obtain melting points presently is by thermodynamic integration, where one starts with some reference system such as the ideal gas where the free energy is known, and then slowly varies the temperature and pressure until the desired liquid state at P and T is reached. This would be difficult for ionic systems, however, where there is no ergodic ideal reference state for the charged system. [One could use the ionic charge itself as the integration parameter, and slowly vary the charge until the final charged state is reached. However, this would require many simulations to integrate accurately from a reference state of such different character than the final state.]

Cohen and Gong [1994] predicted the melting curve of MgO to 300 GPa using molecular dynamics simulations for finite clusters. The interactions among atoms were obtained using the non-empirical Potential Induced Breathing (PIB) model which had been shown previously to give excellent agreement with experiment for thermoelastic properties of MgO to high pressures [*Isaak, Cohen, and Mehl, 1990*]. Molecular dynamics simulations using the closely related VIB (Variationally Induced Breathing) model (described below) show exceptional accuracy for the equation of state of MgO, including high order

properties such as the change in thermal expansivity with pressure [Inbar and Cohen, 1995]. Given the accuracy of the model for properties of the solid, it was surprising when the first experimental measurements for the melting curve of MgO showed a discrepancy of over a factor of three in the dT/dP slope, with the experiments showing a much shallower slope [Zerr and Boehler, 1994]. Since the MD and lattice dynamics calculations showed that crystalline properties of MgO were well predicted by the models, such a large discrepancy could indicate a problem with the liquid simulations. Since the potentials do not use any information that is particular to the crystalline state and are based on fundamental physics, only one possibility seemed open—that there was a problem with the liquid simulations due to the use of finite clusters. Cohen and Gong [1994] used finite clusters of 64 to 1000 atoms and then extrapolated to the bulk; they found that the finite cluster results were linear functions of $1/L$, where L is the length (i.e. linear dimension) of the clusters, so they extrapolated T_m with $1/L \rightarrow 0$. The extrapolation to bulk is effectively over about 20 orders of magnitude of system size, so that there is cause for concern that this could introduce errors in the predicted melting curve. Thus here we have effectively eliminated size effects by using another technique based on similar potentials, but with periodic boundary conditions and no surfaces, to obtain the melting slope.

We also further continue the study of melting in clusters using PIB, and look for dynamical premelting effects by computing and studying the power spectrum $S(q,\omega)$ in the crystalline phase. Cohen and Gong [1994] found evidence of an intrinsic instability in the crystal near melting by studying the Lindemann ratio u_{rms}/a where u_{rms} is the r.m.s. displacement and a is the mean near neighbor distance. They found this ratio to be constant along the melting curve spanning 300 GPa and 15,000 K. Whereas such scaling is expected in power law potentials [Ross, 1969] where liquid and solid structures are constant along the melting curve, it is not constrained to behave thusly with realistic potentials. The large changes in liquid structure along the melting curve indicate that the constancy of the Lindemann ratio must have a deeper origin. Cohen and Gong [1994] hypothesized that in pure systems such as MgO, there might be an underlying instability in the crystal leading to melting. The fact that melting is a first-order transition in no way negates this possibility; for instance, there is universal agreement that there is an underlying and observable overdamped soft mode in BaTiO₃, in spite of the fact that its ferroelectric transitions are first-order. They proposed a similar scenario for MgO, but there was no evidence of what the underlying instability might be. The best candidate is the shear instability $c_{11}-c_{12}$, which vanishes at the melting point at zero pressure, but the instability occurs at higher temperatures than the melting point with increasing pressure; the meaning of this behavior is still a mystery. Here we try to understand better whether there is an underlying dynamical instability

in the lattice and what it is by studying the dynamical structure factor or power spectrum $S(q,\omega)$ in crystalline clusters of 1000 atoms as melting is approached.

Much work has been done on premelting in clusters and finite systems concentrating on surface melting and roughening transitions [*Bastiannsen and Knops*, 1996; *Nagaev and Zil'berverg*, 1996]. There is also considerable evidence that small clusters do not undergo discontinuous phase transitions, but rather go through a region of fluctuations between solid-like and liquid-like configurations [*Bhattacharya, Chen, and Mahanti*, 1996; *Nayak, Ramaswamy, and Chakravarty*, 1995; *Wells and Berry*, 1994]. Our 1000 atom clusters are significantly larger than those discussed in the latter studies, which range up to 55 atoms. Evidence was seen in Cohen and Gong [1994] for coexistence and slow fluctuations between solid and liquid in the van der Waals loop region of the transition, which is probably closely related to what is observed in the smaller clusters. Our interest in studying $S(q,\omega)$ is not however to understand better the dynamics of this fluctuation/coexistence regime, but rather to look for evidence of an approaching dynamical instability in the crystalline field as the melting point is approached.

Methods

We performed classical molecular dynamics simulations for periodic and cluster systems, using the non-empirical VIB and PIB models, respectively. VIB [*Wolf and Bukowinski*, 1988] and PIB [*Cohen, Boyer, and Mehl*, 1987a] are very similar ionic Gordon-Kim [*Gordon and Kim*, 1972] type models, in which the total charge density is modeled by overlapping ionic charge densities, which are computed from quantum mechanical atomic calculations with no adjustable parameters. Only the ionic charge and nuclear charge are input, and the ionic charges used are the nominal 2+ and 2- for Mg and O, respectively. In Gordon-Kim models, the total energy is a sum of three terms, the long-range electrostatic or Madelung energy, the self-energy of each atom or ion, and the short-range interaction energy which is a sum of the kinetic energy, short-range electrostatic, and exchange-correlation energy, all of which are functions of the model charge density. We use the Hedin-Lundqvist [*Hedin and Lundqvist*, 1971] parametrization of the exchange-correlation energy and the Thomas-Fermi kinetic energy in the interaction energy. For the self-energies we use the Kohn-Sham total energy [*Kohn and Sham*, 1965].

Since O^{2-} is not stable in the free state, it is stabilized with a sphere of +2 charge (called a ‘‘Watson sphere’’) in the atomic calculations, and the radius of this sphere is chosen different in the PIB and VIB models; this is the only difference between PIB and VIB. In the PIB model, the radius of the Watson sphere, r_{Wat} is chosen so that the electrostatic potential inside the sphere is the same

as the Madelung (i.e. electrostatic) potential at the site the crystal in order to model the electrostatic stabilization of the O^{2-} ion by the crystal field. In the VIB model, r_{Wat} is chosen to minimize the total energy in the crystal for a given configuration of atoms. Both VIB and PIB give very similar results except at very high pressures where the VIB potential is softer and more accurate due to the fact that it includes short-range contributions to the O^{2-} size, as well as the long-range Madelung contributions [Inbar and Cohen, 1995]. They also give different LO-TO splittings; VIB gives the rigid ion LO-TO splitting whereas PIB gives reduced values that are closer to experiment (although for the wrong reasons) when a simple correction to reference the Madelung potential to the local average potential is included. This is due to the dependence in PIB of r_{Wat} on the magnitude of the potential, as opposed to potential differences [Cohen, Boyer, and Mehl, 1987a, 1987b]. Since the VIB model is better behaved we used the VIB choice of r_{Wat} here for the periodic boundary condition computations. We employ the pair approximation, and calculate pairwise interactions as functions of the distance between atoms and r_{Wat} on the anions, and fit an analytic function to the calculated energies as functions of distance and r_{Wat} . This function, which has up to 21 parameters for O-O interactions, can be evaluated much more rapidly than doing the full quantum calculations at each time step. The resulting potential has been severely tested for thermal properties of MgO [Isaak et al., 1990; Inbar and Cohen, 1995], and we have great confidence in the potential.

In the molecular dynamics simulations, Newton’s equation $\mathbf{F} = \mathbf{ma}$ is integrated forward in time. In VIB, the energy is minimized with respect to all of the \mathbf{r}_{Wat} for each time step. In PIB, the Madelung potentials are computed at each time step. In both cases, the forces are obtained analytically for each configuration of atoms and Watson sphere radii r_{Wat} . The pair interactions and the self-energies of the O^{2-} anions are functions of r_{Wat} for each anion.

Melting Curve

We have simulated crystalline and liquid MgO with periodic boundary conditions, i.e. with no surfaces, using the VIB model to obtain the melting curve. Periodic boundary conditions introduce long-range lattice structure onto a liquid, which should not be present, and this can cause systematic errors especially in ionic crystals with long-range forces. However, by studying two very different periodic cell sizes, 64 atoms, and 512 atoms, we can test whether the quantities we calculate, V and T for given P and E, are affected. We obtain the change in enthalpy and volume, $\Delta H = \Delta E + P\Delta V$ and ΔV , as functions of T and P between the solid and liquid, which at the melting point T_m gives us the

melting slope through the Clapeyron equation,

$$dT/dP = \frac{T_m \Delta V_m}{\Delta H_m}. \quad (1)$$

Since the primary discrepancy with experiment is the melting slope, and both theory and experiment agree on the melting point at zero pressure, we fix the zero pressure melting point at 3200K and then integrate the Clapeyron equation to give the melting curve.

In the periodic boundary condition simulations, we employed the variable-cell-shape technique of Parinello and Rahman[1980], in which extra fictitious dynamical degrees of freedom associated with the shape of the computational cell are introduced to allow the computational cell volume and shape to vary. This technique conserves enthalpy, rather than energy, and the external pressure is kept constant, rather than the volume. The off-diagonal elements of the strain matrix were not allowed to vary to avoid problems with large fluctuations in the shape of the periodic cell in the liquid state.

The systems consisted of a sample of 64 atoms, initially arranged in a cubic lattice. In order to check for system-size effects, some simulations were also carried out on a 512- atom system. Periodic boundary conditions were employed to eliminate surface effects, and a timestep of 1 fs was selected. The equations of motion were numerically integrated using a fifth-order Gear Predictor-Corrector method [Gear, 1966]. Throughout our simulations, enthalpy was conserved to approximately 1 part in 10^6 per iteration.

Simulations were performed at $P= 0, 12.5, 25, 50$ and 100 GPa. At each pressure, MD runs were performed at various temperatures near the expected melting point in both solid and liquid. Initially, the kinetic energies of the atoms were scaled to obtain approximately the desired temperature. After equilibration, which lasted for 2 ps, we ran each simulation for an additional 6-15 ps during which the system volume, enthalpy, and kinetic energy were monitored each iteration. The length of each run was determined by the convergence of the average volume of the system. The enthalpy was a constant of the motion. The temperature was calculated from the average kinetic energy, and the volume averaged.

After performing these simulations at several temperatures in the solid, the limit of superheating was reached, and the solid melted. This was determined both from the presence of diffusion, and the dramatic reduction in intensity of a simulated Bragg reflection intensity. After melting, the temperature dropped because of the conversion of the latent heat of melting to potential energy. Similar simulations were performed in the liquid.

Power Spectrum

Since the previous cluster calculations [Cohen and Gong, 1994] used PIB as opposed to VIB, we use PIB here for the study of the dynamic structure factor $S(\mathbf{q}, \omega)$ in clusters. The power spectrum $S(\mathbf{q}, \omega)$ was obtained as follows. Simulations for clusters of 1000 atoms were performed for MgO at $P=0, 100$ and 150 GPa at a series of temperatures. At zero pressure the cluster had free boundary conditions, and for the high pressure runs pressure was imposed by enclosing the cluster in a cubic elastic box as in Cohen and Gong. Atoms that hit the box walls reflect specularly; the momentum component perpendicular to the wall is reversed. The Verlet algorithm was used to integrate the classical Newton's equations with a time step of 2 fs. Simulations were started with equilibrated system prepared by Cohen and Gong [1994] and were run for 20,000 time steps. Frames of the atomic positions were saved every 8 time steps for computation of $S(\mathbf{q}, \omega)$. The density function ρ is defined as

$$\rho(\mathbf{r}, t) = \sum_{i=1}^N \delta(\mathbf{r} - \mathbf{r}_i(t)) \quad (2)$$

and the transform is

$$p(\mathbf{k}, t) = \sum_{i=1}^N e^{i\mathbf{k} \cdot \mathbf{r}_i(t)}. \quad (3)$$

The dynamical structure factor is defined as

$$S(\mathbf{q}, \omega) = \int dt F(\mathbf{q}, t) e^{i\omega t} W(t) \quad (4)$$

where $\mathbf{q} = 2\pi\mathbf{k}/l$ for mean cubic cell lattice constant l and $F(\mathbf{q}, t)$ is the intermediate structure function defined as the correlation function

$$F(\mathbf{q}, t) = \langle p(\mathbf{q}, t) p^*(\mathbf{q}, 0) \rangle \quad (5)$$

where $\langle \rangle$ indicates an average over all time origins. We used the Blackman-Harris exact three parameter window function [Harris, 1978]

$$W(t) = 0.42659071 + 0.49656062 \cos(2\pi t/T) + 0.07684867 \cos(4\pi t/T) \quad (6)$$

where T is the total time in order to minimize artifacts from the finite time series. Eq. 4 is solved by a discrete fast Fourier transform over the time slices. In order to improve statistics [Press et al., 1992] runs were divided into eight segments and seven overlapping transforms were performed and averaged.

We also averaged over equivalent q 's and the final $S(\mathbf{q}, \omega)$ was smoothed with a running average over $\pm 1 \text{ cm}^{-1}$.

There are non-trivial issues regarding \mathbf{q} dependent quantities such as $S(\mathbf{q}, \omega)$ for clusters. In periodic boundary conditions, the meaningful \mathbf{q} -space is quantized according to the size of the periodic cell. However in a cluster, results can be obtained for any \mathbf{q} . This is because we have free boundary conditions at the surfaces so that the waves do not need to have nodes at the surfaces. However for almost all \mathbf{q} 's, there is a large peak at $S(q, \omega = 0)$ due to the fact that there are not equal numbers of positive and negative displacements for most \mathbf{q} 's. At these \mathbf{q} 's it is difficult to obtain a clear spectrum of $S(q, \omega)$ because aliasing and spillout of the $\omega = 0$ peak results from the finite time sampling and windowing, thus masking the physically important behavior at small ω . Thus we pick \mathbf{q} 's that are minima in $S(q, 0)$, and these turn out to be close to the commensurate \mathbf{q} 's at $(\frac{q}{2}, \frac{q}{2}, \frac{q}{2})$, $(qq0)$, and $(q00)$ where $q = 0.1, 0.2, 0.3, 0.4, \text{ and } 0.5 \cdot 4\pi/a$ where a is the cubic lattice constant (note that for an fcc lattice the X point is at $(2\pi/a, 0, 0)$ and the L point is at $(\pi/a, \pi/a, \pi/a)$ where a is the cubic lattice constant). A further complication is that at finite temperatures the minima are sharp single peaks along $(q00)$, sharp double peaks along $(qq0)$, and sharp triple peaks along (qqq) due to the thermal motions. Thus we displaced our choice of \mathbf{q} slightly from the commensurate \mathbf{q} 's to obtain the best spectra. When q is in the first Brillouin zone $S(\mathbf{q}, \omega)$ gives to first order only the longitudinal excitations since the particle positions enter only as $q \cdot r$ [Kaneko and Ueda, 1989], thus we do not expect to see clear peaks for transverse excitations. The complexity of our spectra may reflect the fact that we are looking primarily at longitudinal excitations, which are affected greatly by electrostatic depolarization effects in finite crystals.

Results and Discussion

Melting Curve

Results of our simulations showing the enthalpies and volumes of solid and liquid at $P = 0$ are shown in fig.1. As a check on system-size effects, the calculations were repeated using a 512-atom system. No system-size effects were seen in volume or enthalpy. For any temperature, one may obtain the difference in volume and enthalpy between solid and liquid, either by interpolating or extrapolating. From the figure one can see that there is some temperature variation in both of these quantities. However, because both are increasing functions of temperature, their quotient is less sensitive.

To obtain the melting curve, the melting temperature at each pressure was estimated to be the temperature of the liquid just beyond the limit of superheating of the solid. ΔV and ΔH of melting

were then calculated for those temperatures, and Eq. 1 numerically integrated to obtain new estimates of the melting temperatures. This process was repeated until the melting temperature converged. The resulting melting curve is shown in fig. 2.

We show the fractional change in volume on melting and ΔH_m versus pressure in fig. 3. Agreement is quite good for the volume of melting with Cohen and Gong [1994] and with Vocadlo and Price [1996]. The enthalpy of melting agrees within the precision of the earlier cluster results of Cohen and Gong. The ΔH_m of Vocadlo and Price are in good agreement with our results at zero pressure, but show a drop with increasing pressure. We consider it more likely for ΔH_m to increase with pressure as we find, since ionic interaction energies increase with pressure and thus it should take more energy to diffuse atoms or disorder the system on melting for ionic forces.

There is a large discrepancy between our predicted melting curve and the experimental melting results of Zerr and Bohler, amounting to a factor of three in the slope dT/dP (114 K/GPa versus 35, respectively). This implies a discrepancy in ΔV_m and/or ΔH_m through the Clapeyron equation (eq. 1). Unfortunately, neither ΔH_m nor ΔV_m have been measured directly for any alkaline earth oxide. Nevertheless, our value for ΔH_m is consistent with literature estimates [Chase, 1985]. However, even in principal we could not prove that the experimental result is incorrect using a theoretical model; rather further experiments are called for. One possible explanation of the origin of the discrepancy would be Ar solubility in the MgO melt in the experiments, thus depressing the melting curve at high pressures. Other issue would be the melting criterion which perhaps is more difficult at non-zero pressure. In any case finding the origin of the discrepancy is important since similar methods are being used to obtain melting curves for other materials as well.

Power Spectrum

The power spectrum $S(q, \omega)$ is quite complicated for our clusters and is not fully understood. The complication over periodic boundary conditions is that we observe not only phonon-like excitations, but also free oscillations of the cluster [Ozaki, Ichihashi, and Kondow, 1991], which are particularly evident at zero pressure due to the free surfaces. Fig. 4 shows the power spectrum as a function of q at zero pressure. The dispersive peaks are phonon-like modes and those whose frequencies vary little with q are the free oscillations. The latter are most obvious at the smallest q since at small q the response is effectively averaged over the whole cluster. Similar behavior was observed in tiny Ar_{13} clusters [Bhattacharya, Chen, and Mahanti, 1996]. The phonon peaks are also split due to the shape of the cluster and its small finite size. Finally, as mentioned above, we expect to primarily see only

longitudinal motions as we have only considered q in the first Brillouin zone. The frequencies obtained using lattice dynamics in periodic boundary conditions at the average volume of the cluster at zero pressure (21 \AA^3) are indicated by the straight line segments. It is clear from the complicated spectra and the complex relationship (or lack thereof) between the peaks in $S(q, \omega)$ and periodic boundary conditions that the cluster, at least at zero pressure, has a significantly different mode structure than a periodic crystal. This must be kept in mind when interpreting our results. Until a similar study is done in periodic boundary conditions we must consider the behavior of the power spectrum we obtain to indicate properties of clusters, not necessarily bulk MgO.

In any case, we do observe interesting behavior in the cluster $S(q, \omega)$ on increasing temperature towards melting. These results are shown in fig. 5. The most obvious changes on increasing temperature are the reduction in intensity of the phonon and free oscillation peaks, and significantly before the melting transition growth is observed in the low frequency response. Fig. 6 shows the low frequency part of the response ($3\text{-}19 \text{ cm}^{-1}$) as a function of temperature. The rapid rise below the melting transition is evidence of premelting behavior which may be related to increases in heat capacity on approach to melting observed in many systems [*Richet and Fiquet, 1991*]. It may also be related to instabilities driven by dislocations in larger systems [*Lund, 1992*].

Since our clusters have surfaces, the first obvious question is whether the low frequency power we observe on approach to melting is related to surface melting or other surface changes, or is in the bulk of the cluster. In order to determine where the low frequency power is localized we filtered the Fourier representation of the density function (eq. 3) and then transformed back to real space. Fig. 7a shows a representative snapshot of resulting low frequency, low q weight contribution on each atom, with the radii of the atoms proportional to their contribution to the low frequency response at 100 GPa and $T=11360 \text{ K}$. It is clear that the low frequency power is a bulk effect and not localized at the surface.

Next we consider what dynamics is involved in the low frequency part of $S(q, \omega)$ by tracing out selected trajectories of atoms, and coloring the trajectories by their contribution to the low frequency power (fig. 7b). If all trajectories were depicted it is difficult to make anything out, but it is clear from examining many trajectories and snapshots that at high pressures the low frequency power is due to complicated many atom exchanges.

Conclusions

We have performed MD simulations of periodic bulk and finite 1000 atom clusters of the melting of MgO. We obtain a melting curve that has a slope three times greater than that obtained experimentally,

but obtain reasonable volumes and enthalpies of melting. The experiments should be repeated. If indeed the ionic model is as far off from experiment as the current results show, something exotic must occur in the electronic structure and bonding of MgO liquid. The alternative is that there is some systematic error in the experiment. We have also studied the power spectrum on heating in MgO clusters and find evidence for premelting phenomena involving many atom exchanges. It is possible that the onset of these many atom exchanges helps lead to the melting instability, or put another way to the thermodynamic destabilization of the crystal.

Acknowledgments

We thank Iris Inbar and Joe Feldman for helpful discussions. Mark Kluge performed the periodic bulk simulations. This work was supported by NSF EAR-9418934, and computations were performed at the Carnegie Institution of Washington and on the CM-5 at the National Center for Supercomputing Applications.

Figure Captions

Figure 1. Volumes and enthalpies of crystalline and liquid MgO as functions of temperature at different pressures. The open diamonds and triangles are for 512 atom supercells; other symbols are for 64 atom supercells. The agreement for the different size periodic systems indicates that we are converged for the volume and enthalpy. ΔV and ΔH are indicated at 0 GPa and 100 GPa respectively. (a) volume, (b) enthalpy.

Figure 2. Melting curve for MgO. The present curve is computed from the MD VIB volume and enthalpy data by integrating the Clapeyron equation (eq. 1) starting at 3200 K at 0 GPa. The Cohen and Gong [1994] curve was obtained by reversing the melting transition for clusters and extrapolating to infinite system size using the PIB model. The Vocadlo and Price [1995] curve was obtained by melting periodic systems with an empirical potential. There is almost perfect agreement between the current results and the Vocadlo and Price results. There is a factor of three discrepancy in the slope with the experimental results of Zerr and Boehler.

Figure 3. Fractional (a) volume of melting and (b) enthalpy of melting versus pressure.

Figure 4. $S(q, \omega)$ for $P=0$ as a function of \mathbf{q} . The sharp low frequency peaks at 60 and 100 cm^{-1} are resonances of the cube. Acoustic phonons are visible at higher frequencies and are dispersive. (a) $(q00)$ (b) $(qq0)$ (c) (qqq) .

Figure 5. $S(q, \omega)$ for $q = (2\pi/5a, 2\pi/5a, 0)$ at (a) 0 GPa, (b) 100 GPa, and (c) 150 GPa. The curves are offset for each temperature shown. At 0 GPa, the crystal has not yet melted at 3200 K, but the low frequency peak is evident. At 100 GPa, melting occurs between 11360 and 11600 for this cluster size, and a low frequency peak arises before melting. At 150 GPa melting occurs between 12800 and 13300K, and there is a low frequency peak at 12800 K.

Figure 6. Low frequency power (integrated from 3-19 cm^{-1}) as a function of temperature at different pressures. At the melting transition the low frequency power seems to drop. Note that melting requires superheating at zero pressure, but little hysteresis is observed at high pressures. Also, note that melting occurs at higher temperatures than the bulk at high pressures.

Figure 7. (a) Representation of selected atomic contributions to the low frequency power at 100 GPa and $T=11360$ in the crystal before melting. (b) Representation of trajectories of selected atoms, with the shade chosen to show the contribution to the low frequency power at $P=100$ GPa, and $T=11360$ K. The black trajectories show atoms that do not contribute to the low frequency response—they show only oscillating, non-diffusive motions. Atoms that contribute to the low frequencies response do diffuse and seem to exchange with other atoms in complicated motions; the greater the low frequency

response, the lighter the shade of grey.

References

- Anderson, W.W. and T.J. Ahrens, Shock temperature and melting in iron sulfides at core pressures, *J. Geophys. Res.* *101*, 5627-5642, 1996.
- Bastiannsen, P.J.M. and H.J.F. Knops, Is surface melting a surface phase transition? *J. Chem. Phys.* *104*, 3822-3831, 1996.
- Bhattacharya, A., B. Chen, S.D. Mahanti, Structural dynamics of clusters near melting, *Phys. Rev. E*, *53*, R33-R36, 1996.
- Boehler, R. Experimental constraints on melting conditions relevant to core formation, *Geochim. Cosmochim. Acta*, *60*, 1109-1112, 1996.
- Chase, M.W., Jr., C.A. Davies, J.R. Downey, Jr., D.J. Frurip, R.A. McDonald, A.N. Syverud, in *JANAF Thermochemical Tables*, Third edition, J. Phys. Chem. Ref. Data, *14*, Suppl. 1985.
- Cohen, R.E., L.L. Boyer, M.J. Mehl, Lattice dynamics of the Potential Induced Breathing model: First principles phonon dispersion in the alkaline earth oxides, *Phys. Rev. B*, *35*, 5749-5760, 1987a.
- Cohen, R.E., L.L. Boyer, M.J. Mehl, Theoretical studies of charge relaxation effects on the statics and dynamics of oxides, *Phys. Chem. Minerals*, *14*, 294-302, 1987b.
- Cohen, R.E. and Z. Gong, Melting and melt structure of MgO at high pressures, *Phys. Rev. B*, *50*, 12301-12311, 1994.
- Gear, C.W. The numerical integration of ordinary differential equations of various orders, Argonne National Laboratory, ANL Report #7126, 1966.
- Gordon, R.G. and Y.S. Kim, Theory for the forces between closed-shell atoms and molecules, *J. Chem. Phys.* *56*, 3122-3133, 1972.
- Harris, F.J. On the use of windows for harmonic analysis w/discrete fourier transforms, *Proceedings of the IEEE*, *66*, 51-83, 1978.
- Hedin, L. and B.I. Lundqvist, Explicit local exchange-correlation potentials, *Journal of Physics C*, *4*, 2064-2083, 1971.
- Heinz, D.L., E. Knittle, J.S. Sweeney, Q. Williams, R. Jeanloz, High-Pressure Melting of (Mg,Fe)SiO₃-Perovskite, *Science*, *264*, 279-280, 1994.
- Inbar, I. and R.E. Cohen, High pressure effects on thermal properties of MgO, *Geophys. Res. Lett.*, *22*, 1533-1536, 1995.

- Isaak, D.G., R.E. Cohen, M.J. Mehl, Calculated Elastic and Thermal Properties of MgO at High Pressure and Temperatures, *J. Geophys. Res.* 95, 7055-7067, 1990.
- Kaneko, Y. and A. Ueda, Dynamical structure factor of α -AgI, *Phys. Rev. B*, 39, 10281-10287, 1989.
- Kohn, W. and L.J. Sham, Self-consistent equations including exchange and correlation effects, *Phys. Rev.*, A140, 1133-1140, 1965.
- Lund, F. Instability driven by dislocation loops in bulk elastic solids: Melting and superheating, *Phys. Rev. Lett.* 69, 3084-3087, 1992.
- Nagaev, E.L. and V.E. Zil'berverg, Double surface-bulk melting and suppression of overheating at first-order phase transitions, *Phys. Rev. B*, 53, 5011-5014, 1996.
- Nayak, S.K., R. Ramaswamy, C. Chakravarty, 1/f spectra in finite atomic clusters, *Phys. Rev. Lett.* 74, 4181-4184, 1995.
- Ozaki, Y., M. Ichihashi, T. Kondow, Analysis of breathing vibration of nearly spherical Ar clusters based on a dense sphere model, *Chem. Phys. Lett.*, 182, 57-62, 1991.
- Parrinello, M. and A. Rahman, Crystal structure and pair potentials: A molecular dynamics study, *Phys. Rev. Lett.* 45, 1196-1199, 1980.
- Press, W.H., S.A. Teukolsky, W.T. Vetterling, B.P. Flannery, in *Numerical Recipes in FORTRAN: The Art of Scientific Computing*, , Second edition, Cambridge University Press, New York, p. 549, 1992.
- Richet, P. and G. Fiquet, High-temperature heat capacity and premelting of minerals in the system MgO-CaO-Al₂O₃-SiO₂, *J. Geophys. Res.* 96, 445-456, 1991.
- Ross, M., Generalized Lindemann melting law, *Phys. Rev.* 184, 233-242, 1969.
- Sweeney, J.S. and D.L. Heinz, Melting of iron-magnesium-silicate perovskite, *Geophys. Res. Lett.* 20, 855-858, 1993.
- Sweeney, J.S. and D.L. Heinz, Irreversible Melting of a Magnesium-Iron-Silicate Perovskite at Lower Mantle Pressures, [abstract] *EOS Trans. Am. Geophys. Union*, 76, F553, 1995.
- Wells, D.J. and R.S. Berry, Coexistence in finite systems, *Phys. Rev. Lett.*, 73, 2875-2878, 1994.
- Wolf, G.H. and M.S.T. Bukowinski, Variational stabilization of the ionic charge densities in the electron-gas theory of crystals: Applications to MgO and CaO, *Phys. Chem. Minerals*, 15, 209-220, 1988.

Zerr, A. and R. Boehler, Melting of (Mg,Fe)SiO₃ perovskite to 625 kilobars: indication of a high melting temperature in the lower mantle, *Science*, 262, 553-555, 1993.

Zerr, A. and R. Boehler, Constraints on the melting temperature of the lower mantle from high-pressure experiments on MgO and magnesiowustite, *Nature*, 371, 506-508, 1994.

Received _____

Fig. 1 Cohen and Weitz

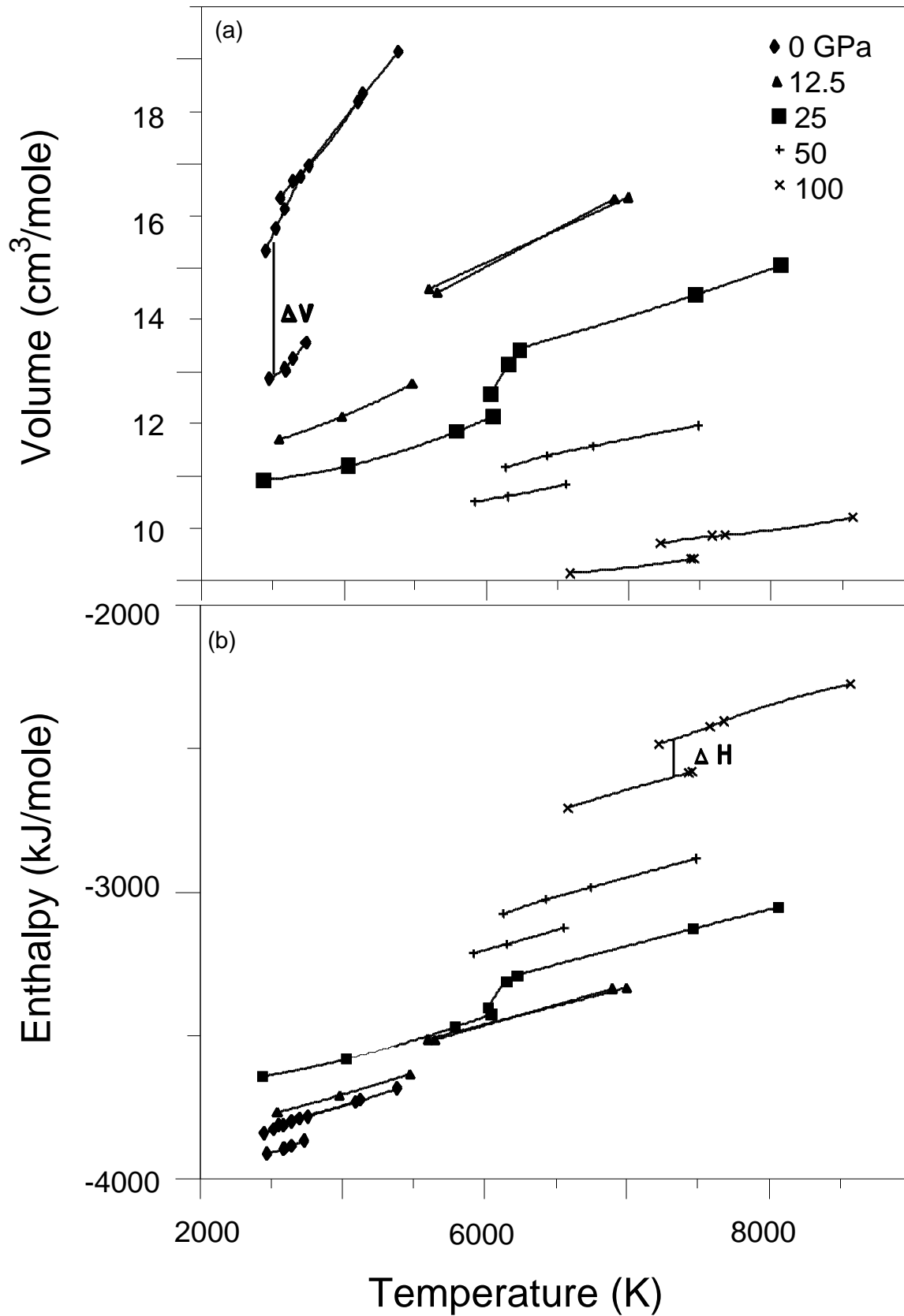


Fig. 2 Cohen and Weitz

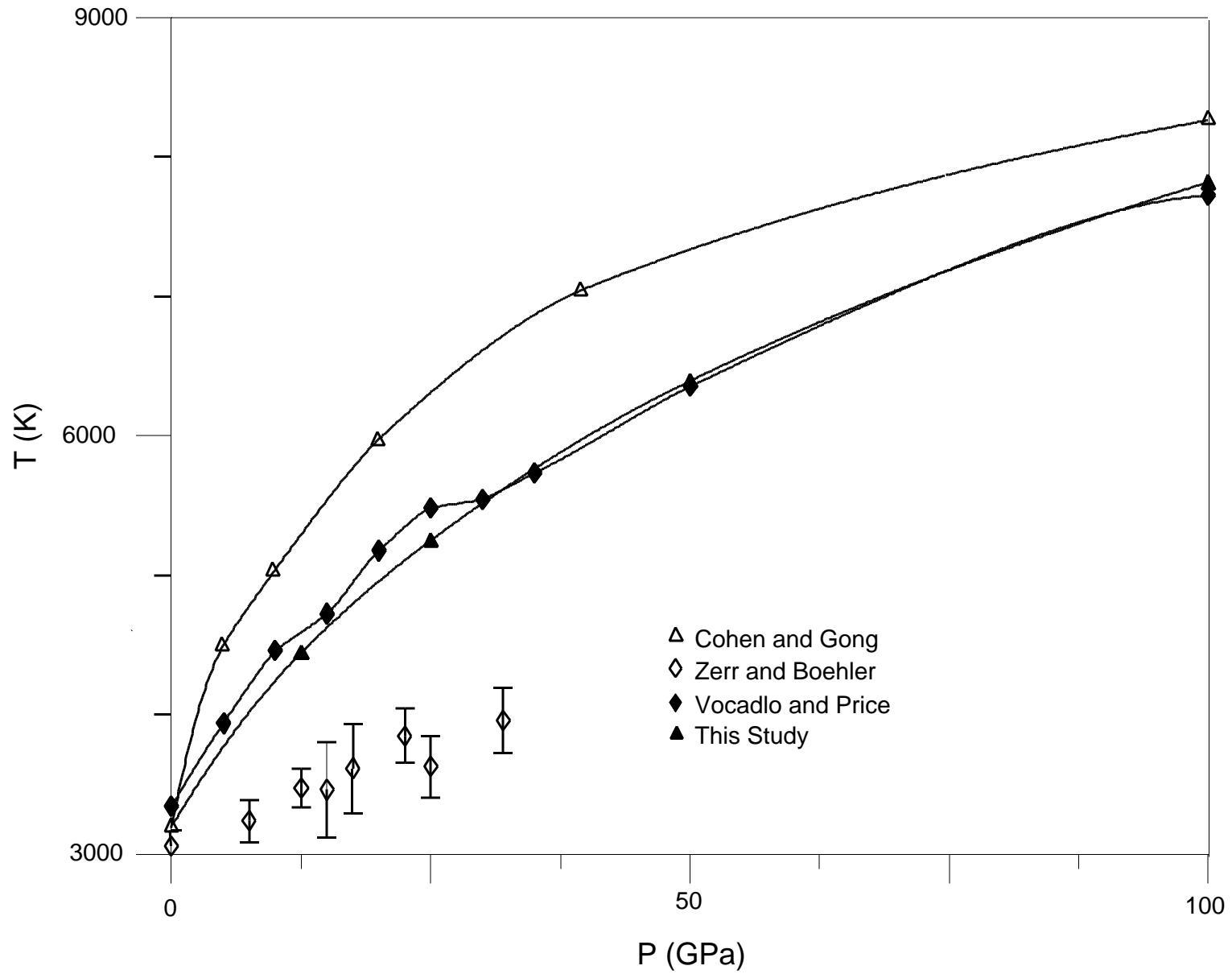


Fig. 3 Cohen and Weitz

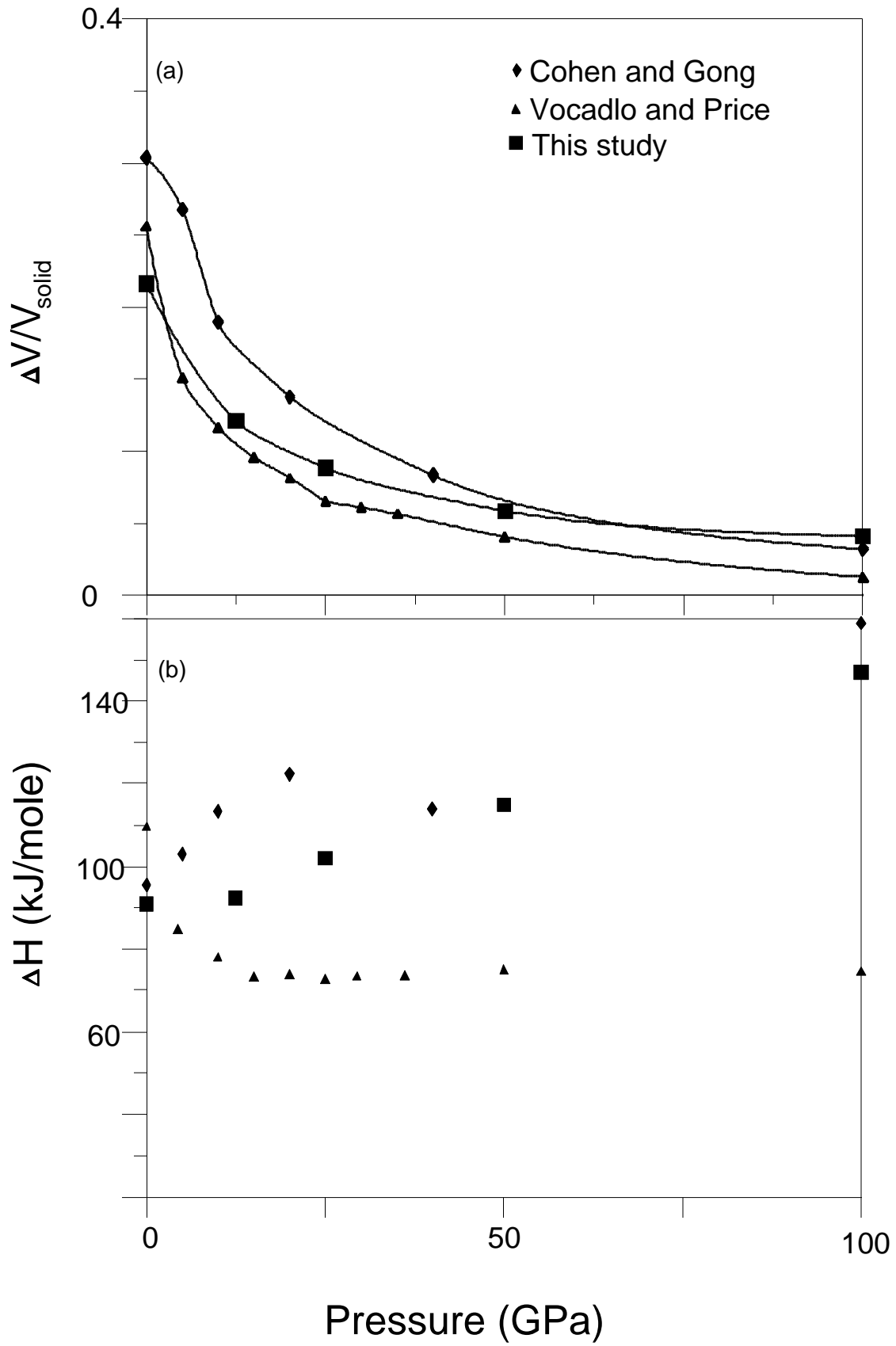


Fig. 4 Cohen and Weitz

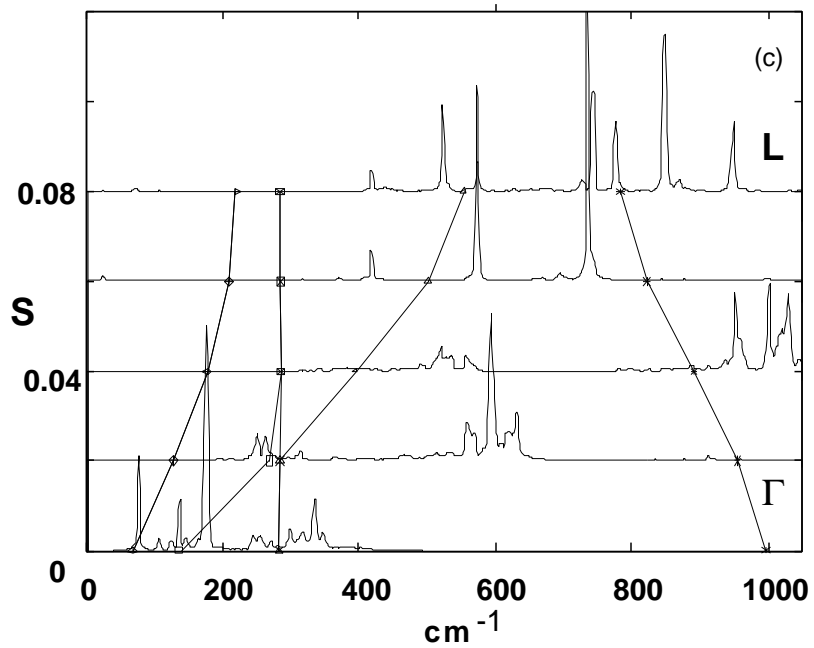
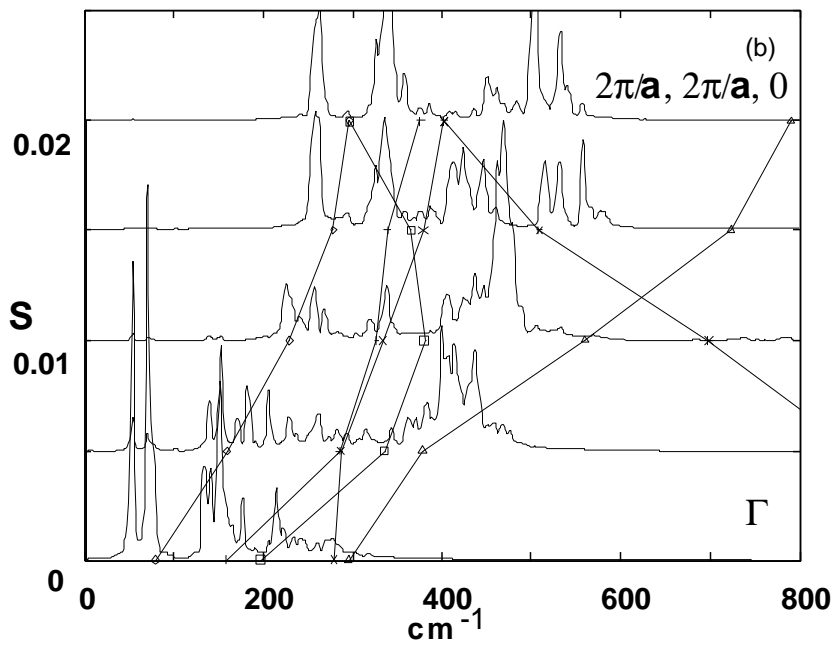
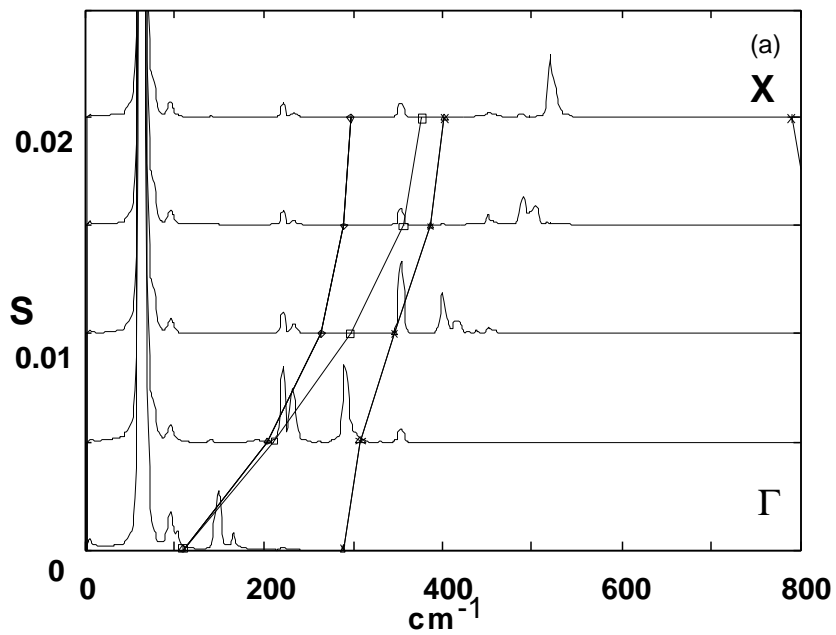


Fig. 5 Cohen and Weitz

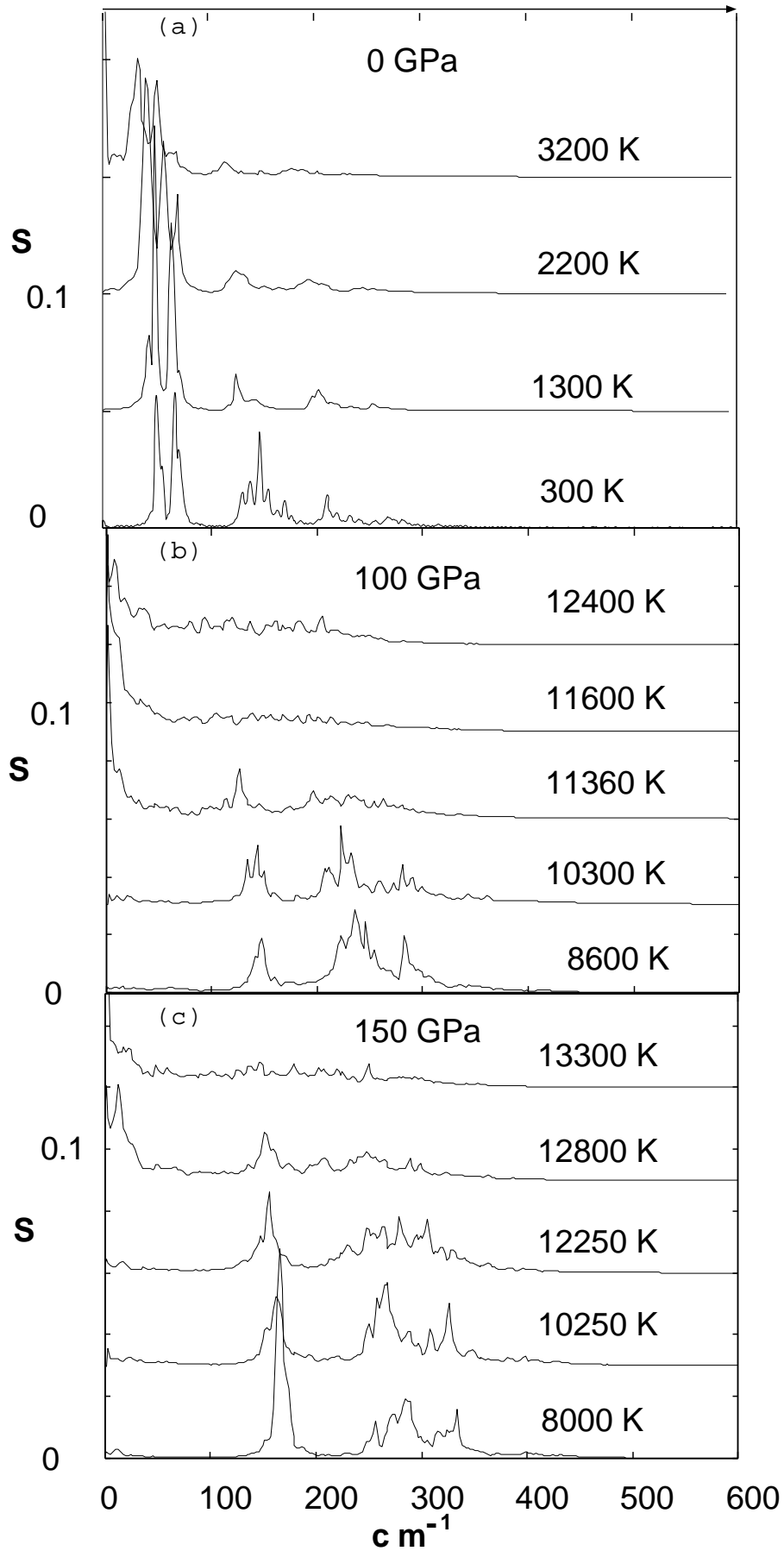


Fig. 6 Cohen and Weitz

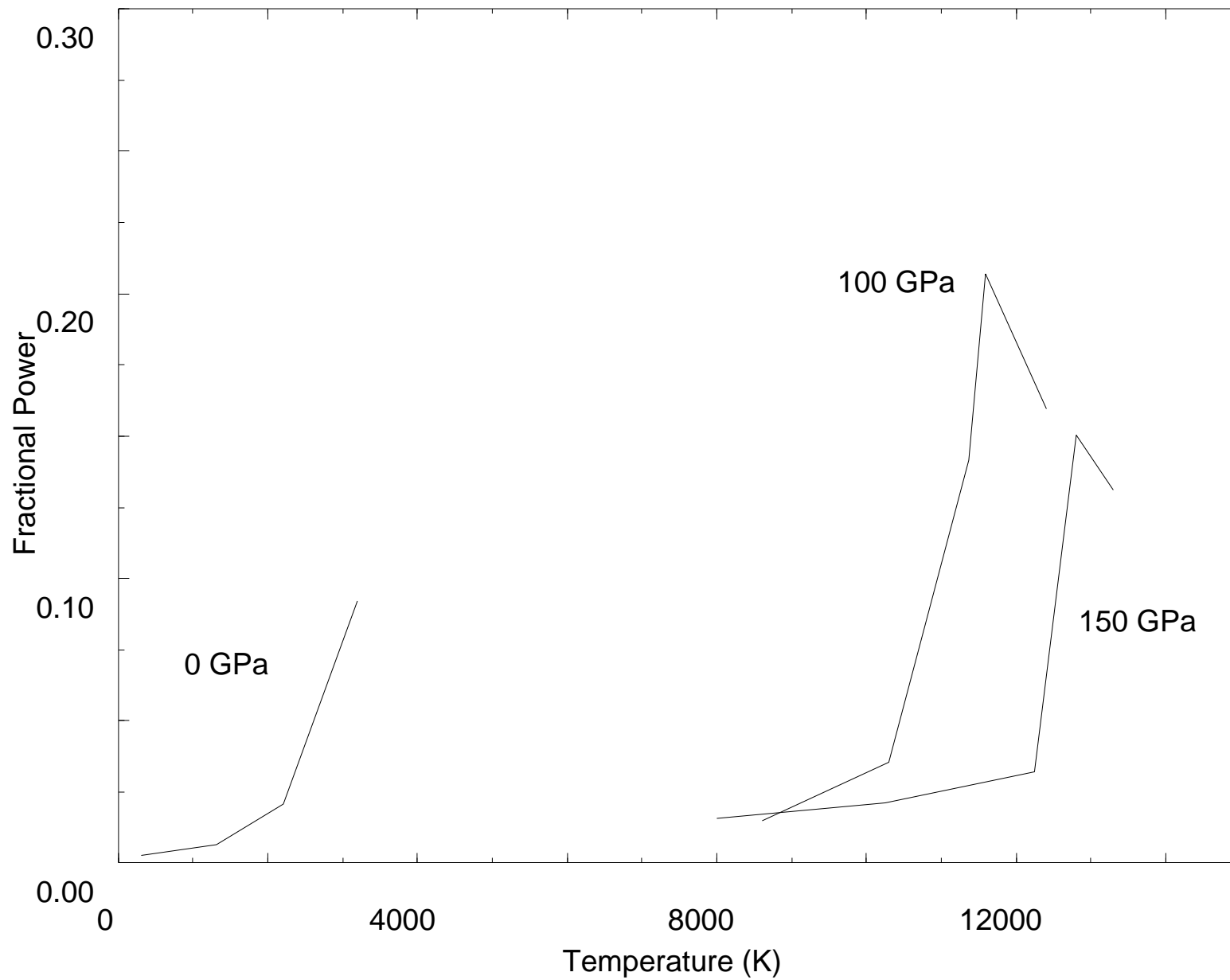
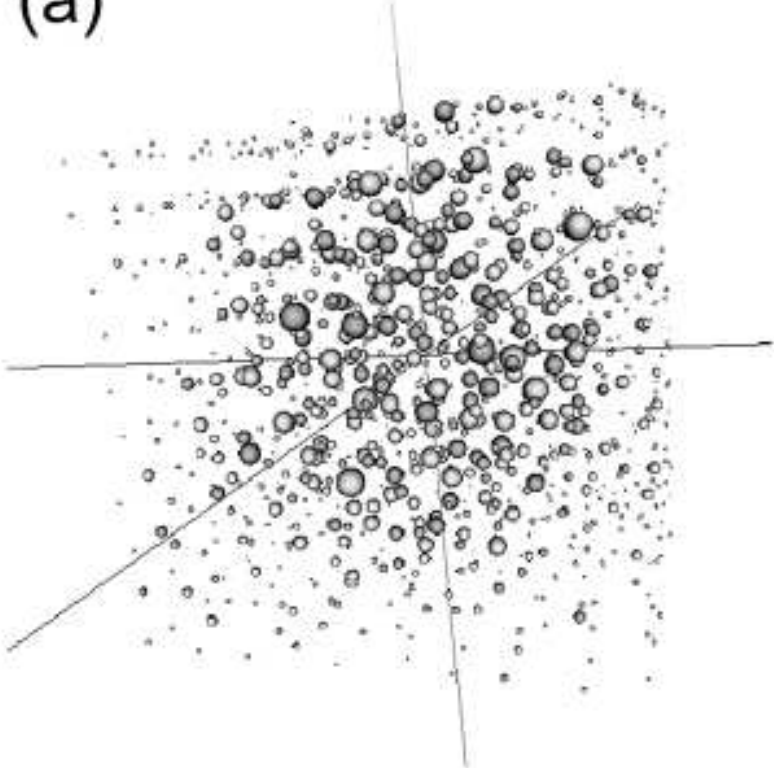


Fig. 7 Cohen and Weitz

(a)



(b)

